Chapter 8
Assessing the Effect of Aging on Soil Liquefaction Resistance

Ronald D. Andrus and Barnabas Bwambale

8.1 Introduction

The resistance of soil to liquefaction is often expressed by the cyclic resistance ratio (*CRR*) estimated from semi-empirical charts based on field tests, such as the cone penetration test (CPT), standard penetration test (SPT) or shear wave velocity (V_S) measurement (e.g., Youd et al. 2001; Idriss and Boulanger 2008; National Academies of Sciences 2016). Commonly used *CRR* charts are derived from primarily field case histories where liquefaction occurred in soil deposits that are less than a few thousand years old (Youd et al. 2001; Idriss and Boulanger 2008; National Academies of Sciences 2016; Hayati and Andrus 2009; Seed 1979; Bwambale and Andrus 2019). If these charts are applied without correction for the effect of aging, excessively conservative estimates of *CRR* might be obtained, leading to unnecessary and costly ground improvements. On the other hand, if older soil deposits are blindly assumed to be unsusceptible to liquefaction, less conservative assessments of the hazard might be obtained.

Aging (or diagenesis) is the post-depositional physical, chemical and biological processes that alter the structure of soil. As discussed by Boggs (2006), physical processes can include rearrangement and interlocking of soil particles, particles crushing and asperity shearing. Chemical processes can include precipitation of quartz, feldspar, carbonate cements, kaolinite or chlorite, and formation of pyrite or iron oxides. Biological processes include the reworking of sediments by living organisms, bacterial oxidation of organic matter and reduction of inorganic matter, and bacterial fermentation. The combination of these processes contributes to the

R. D. Andrus (✉)
Glenn Department of Civil Engineering, Clemson University, Clemson, SC 29634, USA
e-mail: randrus@clemson.edu

B. Bwambale
ECS Southeast, LLP, Fayetteville, NC 28304, USA
e-mail: bbwamba@clemson.edu

T. G. Sitharam et al. (eds.), *Latest Developments in Geotechnical Earthquake Engineering and Soil Dynamics*, Springer Transactions in Civil and Environmental Engineering, https://doi.org/10.1007/978-981-16-1468-2_8

net effect of diagenesis on liquefaction resistance, which can vary significantly even between locations in the same deposit.

The main objectives of this paper are: (1) to emphasize the importance of not blindly assuming older soil deposits to be unsusceptible to liquefaction by reviewing twelve cases of Holocene (<11.5 k years) liquefaction in Pleistocene (11.5 k to 2.6 M years) deposits; and (2) to review nine proposed relationships for estimating the effect of diagenesis on *CRR*. The 12 cases of Holocene liquefaction in Pleistocene deposits were compiled as part of the doctoral dissertation work of Bwambale (2018) and are published here for the first time. A comprehensive review of the proposed procedures for assessing the aging effect on soil liquefaction resistance is presented in the paper by Bwambale and Andrus (2019). Nine selected relationships for correcting commonly used *CRR* charts for the aging or diagenesis effect are summarized in this paper.

8.2 Holocene Liquefaction in Pleistocene Deposits

Although most cases of earthquake-induced liquefaction described in the literature involve soils deposited during the Holocene, several cases involving Pleistocene deposits have been reported. Summarized in Table 8.1 are 12 such cases. These cases are from Argentina, China, Israel, Lithuania, Republic of Karelia and the USA. The cases presented in Table 8.1 involve liquefaction of mainly Pleistocene alluvial/fluvial, beach and lacustrine sediments that are composed predominantly of sand, but also include some silt and silty sand. Sand boils (or sand blows) were observed at nearly all locations.

For the 12 cases summarized in Table 8.1, the liquefying events occurred from a few years to about 15,000 years ago. The time difference between the inferred geologic age and any documented liquefying event is, however, greater than 10,000 years, implying old deposits at the time of liquefaction. Some areas (e.g., South Carolina) have experienced liquefaction during multiple events, as indicated in Table 8.1.

Figure 8.1 presents a map of the world showing the geographical locations of the 12 cases of Holocene liquefaction in Pleistocene deposits summarized in Table 8.1. Half of the cases are from the USA. The other six cases are evenly distributed in the continents of Asia, Europe and South America.

Figure 8.2a, b show histograms of the case histories grouped according to deposit type and geologic age (i.e., time since deposition), respectively. As seen in the figures, 54% of the cases occurred in alluvial/fluvial deposits and 23% in each of the two other deposit types. About 70% of the cases involved deposits that are <100,000 years old; and 30% with age between 200,000 to 500,000 years old at the time of liquefaction. This observation suggests that liquefaction susceptibility varies significantly within Pleistocene deposits, often decreasing as the time since deposition increases. The 12 case histories summarized in Table 8.1 support the need for liquefaction assessments in Pleistocene deposits.

Table 8.1 Field case histories of Holocene liquefaction in Pleistocene deposits

Area	Deposit type	Geologic age (years)	Evidence of liquefaction	Year/time of liquefaction (years)	References
Charleston, South Carolina, USA	Beach, fluvial	33 k to >1,000 k	Sand blows, lateral spreading	1886 Charleston earthquake; 5 earlier events	Dutton (1889), Obermeier et al. (1985), Talwani and Cox (1985), Martin and Clough (1994), Lewis et al. (1999), Crone and Wheeler (2000), Talwani and Schaeffer (2001), Hu et al. (2002), Hayati and Andrus (2008), Heidari and Andrus (2012), Hasek and Gassman (2014)
Thousand Springs Valley, Idaho, USA	Alluvium fan low-energy stream channel fill	Probable 10–15 k	Lateral spread with fissures, buckled sod and sand boils	1983 Borah Peak earthquake	Andrus and Youd (1987), Andrus (1994), Andrus et al. (2004a)
Bluffton, South Carolina, USA	Beach?	Pleistocene	Sand blows	1.96 k	Crone and Wheeler (2000), Talwani and Schaeffer (2001), Obermeier et al. (1987)
Georgetown, South Carolina, USA	Beach	~450 k	Sand blows	1.64 and 5.04 k	Crone and Wheeler (2000), Talwani and Schaeffer (2001), Hu et al. (2002), Obermeier et al. (1987)
Marianna, Arkansas, USA	Fluvial	20 k	Sand blows and dike	5.5 k	Blum et al. (2000), Tuttle et al. (2006)
Mendoza and San Juan Provinces, Argentina	Fluvial, lacustrine and fluvio-lacustrine	Pleistocene to Holocene	Sand boils, sand dikes, cracks and fissures	1861–1997 earthquakes	Perucca and Moreiras (2006)

(continued)

Table 8.1 (continued)

Area	Deposit type	Geologic age (years)	Evidence of liquefaction	Year/time of liquefaction (years)	References
Dead Sea Basin, Israel	Lacustrine	15–70 k	Fluidization and injection of clastic dike	7–15 k	Porat et al. (2007), Jacoby et al. (2015)
Lake, Ladoga, Republic of Karelia	Alluvial and lacustrine	Pleistocene and Holocene	Diapir-like injections and dykes; flame and balls-and-pillows structures and breccia	Late Holocene	Biske et al. (2009)
Eastern Baltic Sea, Lithuania	Glacio-fluvial?	Middle Pleistocene	Sediment deformations	<13 k	Bitinas and Lazauskiene (2011)
Dandridge, Tennessee, USA	Fluvial terrace	203 k $\pm$ 13 k	Fluidization-filled fractures and dikes	<15 k	Hatcher et al. (2012), Hatcher (2015)
Xinglong Village, China	Alluvial	$\geq$ 12 k	Sand boiling, surface cracking	2008 Wenchuan earthquake	Li et al. (2013), Liu-Zeng et al. (2017)

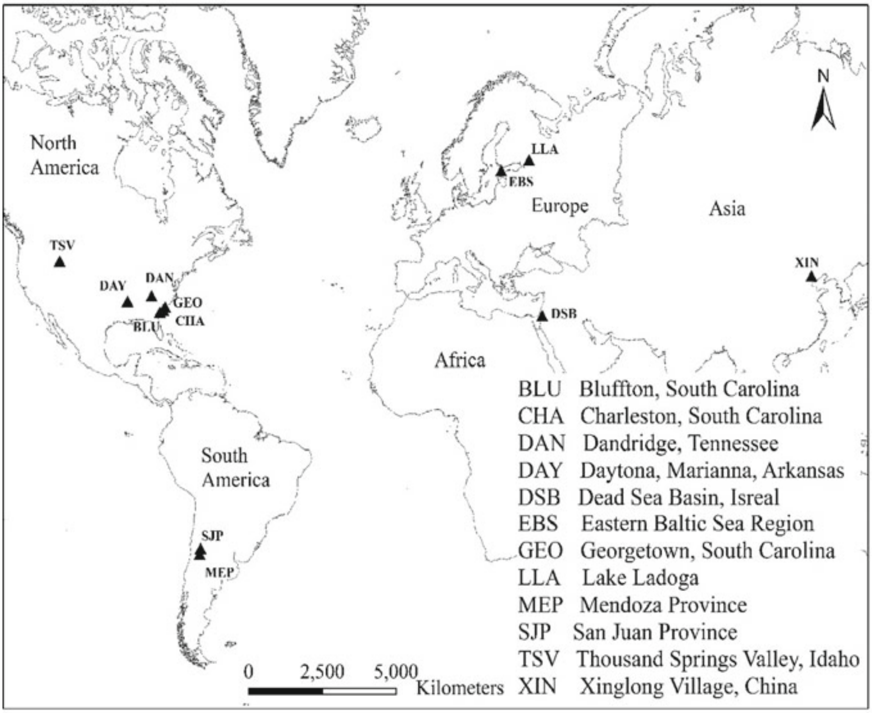

Fig. 8.1 Locations of Holocene liquefaction in Pleistocene deposits

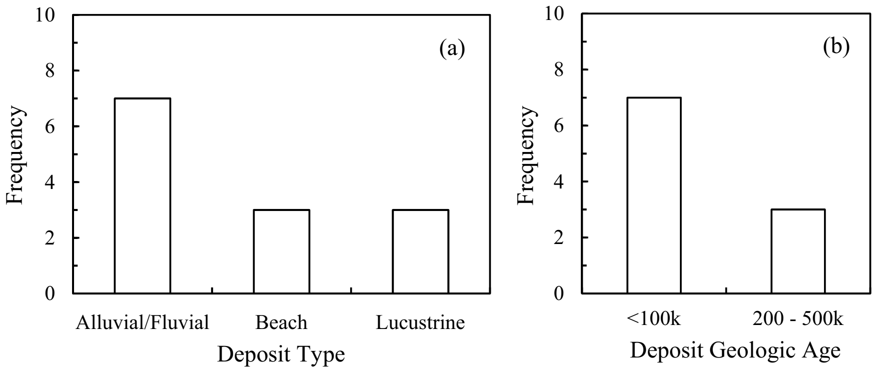

Fig. 8.2 Frequency of cases of Holocene liquefaction in Pleistocene deposits grouped by **a** deposit type and **b** deposit geologic age

8.3 Correcting *CRR* for Diagenesis

The correction of *CRR* for aging or diagenesis can be given by (Hayati and Andrus 2009; Seed 1979; Bwambale and Andrus 2019; Hayati et al. 2008; Arango et al. 2000):

$$CRR_{\text{corrected}} = K_{DR} CRR \tag{8.1}$$

where $CRR_{\text{corrected}}$ is the diagenesis-corrected *CRR*; and K_{DR} is the correction factor. Nine proposed relationships for estimating K_{DR} based on time and a ratio of measured to estimated shear wave velocity are reviewed below.

8.3.1 *Time-*K_{DR} *Relationships*

Because some processes (e.g., liquefaction during strong ground shaking; excavation and backfilling during construction of underground utilities) can cause the grain-to-grain contacts to be broken after deposition, 'time' in this section is defined as the period since the grain-to-grain contacts last formed. This definition of time is sometimes called the 'geotechnical age.' The geotechnical age can be less than the geologic age if an event causes the grain-to-grain contacts to be broken.

Figure 8.3 presents three proposed time-K_{DR} relationships that are primarily based on laboratory cyclic testing of intact and freshly deposited (or reconstituted) specimens composed of predominately silica-based sands. K_{DR} in Fig. 8.3 is defined as the *CRR* of the intact specimen divided by the *CRR* of the reconstituted specimen. The relationship by Seed (1979) is based on test results for five sands. The relationship by Arango et al. (2000) is based on the Seed (1979) relationship and test results for two sands in California and South Carolina. The relationship by Hayati and Andrus (2009) is based on test results for 13 sands in Japan, Taiwan, and the USA. All three relationships suggest a reference age (i.e., time when K_{DR} = 1.0) of <4 days, which is reasonable given that reconstituted laboratory test specimens are typically subjected to back-pressure saturation and consolidation over a period of a few days or less prior to cyclic testing.

Figure 8.4 presents four proposed time-K_{DR} relationships that use a penetration-based *CRR* chart as reference. K_{DR} in Fig. 8.4 is defined as the *CRR* of the intact material divided by the *CRR* from the chart for the given corrected field penetration resistance. The relationship by Hayati and Andrus (2009) is a refinement of the relationship by Hayati et al. (2008) and is based on 24 data points from sites in Canada, Japan, Taiwan and the USA. The relationship by Maurer et al. (2014) is based on the data compiled by Hayati and Andrus (2009) plus data from an area near Christchurch, New Zealand shaken by earthquakes in 2010 and 2011. The relationship by Towhata et al. (2017) is based on field data from Japan, as well as previous studies. The four relationships shown in Fig. 8.4 suggest a reference age

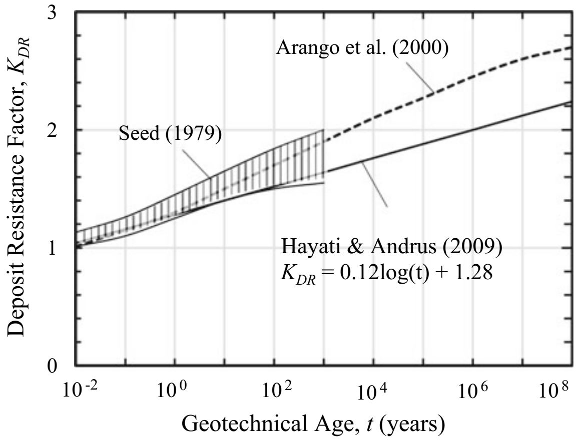

Fig. 8.3 Comparison of three time-K_{DR} relationships based on laboratory testing of silica-based sands (modified from Bwambale and Andrus 2019). K_{DR} is defined as *CRR* of the intact specimen divided by *CRR* of the reconstituted specimen

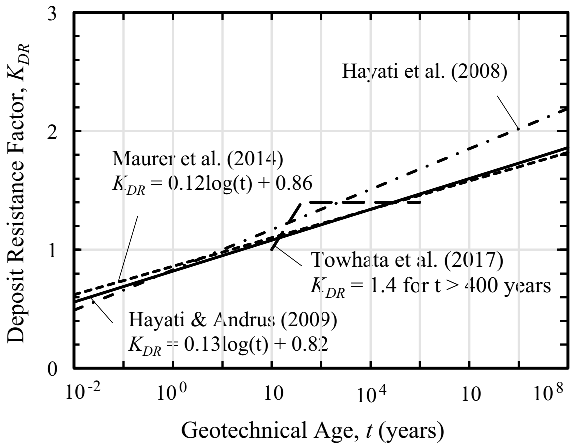

Fig. 8.4 Comparison of four time-K_{DR} relationships based on laboratory and field testing of silica-based sands (modified from Bwambale and Andrus 2019). K_{DR} is defined as *CRR* of the intact material divided by *CRR* from the chart based on penetration resistance

(i.e., time when K_{DR} = 1.0) of 10 to 100 years, which is reasonable given that many case histories used to develop the *CRR* charts are from post-earthquake investigations conducted 1 to 100 years after the liquefying events.

It is encouraging to observe the relationships shown in Figs. 8.3 and 8.4 which indicate similar rates of increase in K_{DR} (12–17%) per log cycle of time. The good agreement is likely because the regression data are from predominately silica-based sands. On the other hand, it should be noted that the results of tailings material reported by Troncoso et al. (1988) were omitted from the regression for the Hayati and Andrus (2009) relationship in Fig. 8.3 because the tailings data exhibit very high values of K_{DR}. Also, K_{DR} values obtained by Bwambale and Andrus (2017) for Pleistocene loess-colluvium near Christchurch, New Zealand plot well above the four relationships in Fig. 8.4. For these reasons, Bwambale and Andrus (2019) do not recommend using relationships based on time unless the rate of increase in resistance in a given deposit is well established.

8.3.2 MEVR-K_{DR} *Relationships*

The ratio of measured shear wave velocity to estimated shear wave velocity (*MEVR*) is a promising predictor variable for K_{DR}. Andrus et al. (2009) recommended using the following relationships for the estimated shear wave velocity (Andrus et al. 2004b, 2009):

$$V_{S1cs,E} = 62.6\left(q_{c1N,cs}\right)^{0.231} \tag{8.2}$$

$$V_{S1cs,E} = 87.6\left[(N_1)_{60,cs}\right]^{0.253} \tag{8.3}$$

where $V_{S1cs,E}$ is the estimated shear wave velocity corrected to a reference stress equal to 100 kPa and a clean-sand equivalent; $q_{c1N,cs}$ is the dimensionless overburden stress-corrected clean-sand equivalent cone tip resistance; and $(N_1)_{60,cs}$ is the dimensionless overburden stress-corrected clean-sand equivalent SPT blow count. Equations 8.2 and 8.3 correspond to deposits with average age of about 6 years (Andrus et al. 2009). In this section, *MEVR* is defined as the measured shear wave velocity ($V_{S1cs,M}$) divided by $V_{S1cs,E}$.

Figure 8.5 presents two proposed *MEVR*-K_{DR} relationships. The relationship by Bwambale and Andrus (2019) is an update to the relationship by Hayati and Andrus

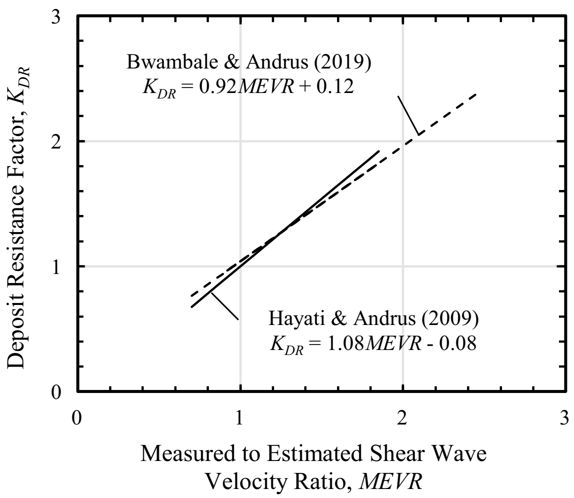

Fig. 8.5 Comparison of two *MEVR*-K_{DR} relationships based on laboratory and field testing, and ground behavior observations. *CRR* from the chart based on penetration resistance is used as reference in the calculation of K_{DR}

(2009). The update involved a critical re-evaluation of the 17 data points compiled by Hayati and Andrus (2009) and the addition of 11 new cases. Nine of the original 17 data points were excluded in the update because of insufficient information, a deficiency in testing procedures and/or a plasticity index too high to be liquefiable. The 20 data points used in deriving the Bwambale and Andrus (2019) relationship are from Canada, Japan, New Zealand, and the USA. $MEVR$-K_{DR} relationships are recommended, instead of time-K_{DR} relationships, because they provide higher coefficients of determination and lower root mean square errors.

8.4 Conclusions

Twelve cases of Holocene liquefaction in Pleistocene deposits were summarized in this paper. The 12 cases are from Argentina, China, Israel, Lithuania, Republic of Karelia and the USA. About 70% of the cases involved deposits that are less than 100,000 years old and 30% with geologic age between 200,000 to 500,000 years old at the time of liquefaction. These cases support the need for liquefaction assessments in Pleistocene deposits.

Nine proposed relationships for correcting the effect of age or diagenesis on *CRR* were reviewed. Although seven time-K_{DR} relationships exhibit similar rates of increase in K_{DR} (12–17%) per log cycle of time for predominately silica-based sands, test results for tailings material and loess-colluvium indicate that much greater rates of increase with time are possible. For this reason, relationships based on measured shear wave velocity to estimated shear wave velocity were recommended for correcting *CRR*.

References

Andrus RD (1994) In situ characterization of gravelly soils that liquefied in the 1983 Borah Peak Earthquake. PhD dissertation, University of Texas at Austin, Austin, TX, pp 246–290

Andrus RD, Youd TL (1987) Subsurface investigation of a liquefaction-induced lateral spread Thousand Springs Valley, Idaho. US Army Corps of Engineers Misc. Paper GL-87-8, Washington, DC

Andrus RD, Stokoe KH, Juang CH (2004a) Guide for shear-wave-based liquefaction potential evaluation. Earthq Spectra 20:285–308

Andrus RD, Piratheepan P, Ellis BS, Zhang J, Juang CH (2004b) Comparing liquefaction evaluation methods using penetration-V_S relationships. Soil Dyn Earthq Eng 24(9–10): 713–721

Andrus RD, Hayati H, Mohanan NP (2009) Correcting liquefaction resistance of aged sands using measured to estimated velocity ratio. J Geotech Geoenviron Eng 135(6):735–744

Arango I, Lewis MR, Kramer C (2000) Updated liquefaction potential analysis eliminates foundation retrofitting of two critical structures. Soil Dyn Earthq Eng 20(1–4):17–25

Biske YS, Sumareva IV, Sheetov MV (2009) Late Holocene paleoseismic event at southeastern coast of Lake Ladoga. I. Principles of research and deformation structures [Russian Source]. Vestnik Sankt-Peterburgskogo Universiteta, Seriya Geologiya i Geografiya 3-25 + 146 + 151

Bitinas A, Lazauskiene J (2011) Implications of the palaeoseismic events based on the analysis of the structures of the Quaternary deposits [Paleoseisminiu ivykiu prielaidos kvartero nuosedu teksturu tyrimo duomenimis]. Baltica 24:127–130

Blum MD, Guccione MJ, Wysocki DA, Robnett PC, Rutledge EM (2000) Late Pleistocene evolution of the lower Mississippi River Valley, southern Missouri to Arkansas. Geol Soc Am Bull 112:221–235

Boggs S Jr (2006) Principles of sedimentary stratigraphy, 4th edn. Pearson Prentice Hall, Upper Saddle River, NJ

Bwambale B (2018) Reducing uncertainty in the assessment of aging effects on soil liquefaction. PhD dissertation, Clemson University, Clemson

Bwambale B, Andrus RD (2017) Liquefaction resistance of pleistocene loess-colluvium deposits near Christchurch, New Zealand. In: 3rd international conference proceedings on performance-based design in earthquake geotechnical engineering (PBD-III), Vancouver, Canada, Paper No. 206

Bwambale B, Andrus RD (2019) State of the art in the assessment of aging effects on soil liquefaction. Soil Dyn Earthq Eng 125:

Crone AJ, Wheeler RL (2000) Data for quaternary faults, liquefaction features, and possible tectonic features in the Central and Eastern United States, east of the Rocky Mountain Front. United States Geological Survey, Denver, CO

Dutton CE (1889) The Charleston earthquake of August 31, 1886. Ninth annual report of the U.S. geological survey 1887–1888, Washington, DC, pp 203–528

Hasek MJ, Gassman SL (2014) Characterization of aged Coastal Plain soils at Hollywood, SC using petrography and microscopy. In: 2014 Geo-congress technical papers, Geo-characterization and Modeling for Sustainability 2088–2097

Hatcher RD Jr (2015) Written communication on the Dandridge liquefaction features to Andrus, R. D 2015/3/13

Hatcher RD Jr, Vaughn JD, Obermeier SF (2012) Large earthquake paleoseismology in the East Tennessee seismic zone: results of an 18-month pilot study. Spec Paper Geol Soc Am 493:111–142

Hayati H, Andrus RD (2008) Liquefaction potential map of Charleston, South Carolina based on the 1886 earthquake. J Geotech Geoenviron Eng 134(6):815–828

Hayati H, Andrus RD (2009) Updated liquefaction resistance correction factors for aged sands. J Geotech Geoenviron Eng 135(11):1683–1692

Hayati H, Andrus RD, Gassman SL, Hasek M, Camp WM, Talwani P (2008) Characterizing the liquefaction resistance of aged soils. Geotech Earthq Eng Soil Dyn IV, GSP 181:1–10

Heidari T, Andrus RD (2012) Liquefaction potential assessment of Pleistocene beach sands near Charleston, South Carolina. J Geotechn Geoenviron Eng 138(10):1196–1208

Hu K, Gassman SL, Talwani P (2002) In-situ properties of soils at paleoliquefaction sites in the South Carolina Coastal Plain. Seismol Res Lett 73:964–978

Idriss IM, Boulanger RW (2008) Soil liquefaction during earthquakes. Earthquake Engineering Research Institute Publication MNO-12, Oakland, CA

Jacoby Y, Weinberger R, Levi T, Marco S (2015) Clastic dikes in the Dead Sea basin as indicators of local site amplification. Nat Hazards 75:1649–1676

Lewis MR, Arango I, Kimball JK, Ross TE (1999) Liquefaction resistance of old sand deposits. In: 11th Pan American conference proceedings on soil mechanics and geotechnical engineering. Foz do Iguassu, Brazil, pp 821–829

Li LH, Fan LF, Deng XL, Hu RL, Zhang J, Wei X (2013) Engineering geological characteristics of sand liquefaction in Wenchuan earthquake. In: Wu, Qi (eds) Global view of engineering geology and the environment. Taylor & Francis Group, London, pp 733–738

Liu-Zeng J, Wang P, Zhang Z, Li Z, Cao Z, Zhang J, Xiaoming Y, Wang W, Xing X (2017) Liquefaction in western Sichuan Basin during the 2008 Mw 7.9 Wenchuan earthquake, China. Tectonophysics 694:214–238

Martin JR, Clough GW (1994) Seismic parameters from liquefaction evidence. J Geotech Eng 120:1345–1361

Maurer BW, Green R, Cubrinovski M, Bradley BA (2014) Assessment of aging correction factors for liquefaction resistance at sites of recurrent liquefaction. In: 10th national conference proceedings on earthquake engineering. Earthquake Engineering Research Institute, Anchorage, AK

National Academies of Sciences (2016) Engineering and medicine: state of the art and practice in the assessment of earthquake-induced soil liquefaction and its consequences. The National Academies Press, Washington, DC

Obermeier SF, Gohn GS, Weems RE, Gelinas RL, Rubin M (1985) Geologic evidence for recurrent moderate to large earthquakes near Charleston, South Carolina. Science, New Series 227:408–411

Obermeier SF, Weems RE, Jacobson RB (1987) Earthquake-induced liquefaction features in the Coastal South Carolina Region. In: Symposium on seismic hazards proceedings, ground motions, soil-liquefaction and engineering practice in Eastern North America, Sterling Forest Conference Center, Tuxedo, New York, pp 480–493

Perucca LP, Moreiras SM (2006) Liquefaction phenomena associated with historical earthquakes in San Juan and Mendoza Provinces, Argentina. Quat Int 158:96–109

Porat N, Levi T, Weinberger R (2007) Possible resetting of quartz OSL signals during earthquakes—evidence from late Pleistocene injection dikes, Dead Sea basin, Israel. Quat Geochronol 2:272–277

Seed HB (1979) Soil liquefaction and cyclic mobility evaluation for level ground during earthquakes. J Geotechn Eng Div 105(2):201–255

Talwani P, Cox J (1985) Evidence for recurrence of earthquakes near Charleston, South Carolina. Science, New Series 229:379–381

Talwani P, Schaeffer WT (2001) Recurrence rates of large earthquakes in the South Carolina Coastal Plain based on paleo-liquefaction data. J Geophys Res 106:6621–6642

Towhata I, Taguchi Y, Hayashida T, Goto S, Shintaku Y, Hamada Y, Aoyama S (2017) Liquefaction perspective of soil ageing. Géotechnique 67(6):467–478

Troncoso J, Ishihara K, Verdugo R (1988) Aging effects on cyclic shear strength of tailings materials. In: 9th world conference proceedings on earthquake engineering, vol III, Tokyo-Kyoto, Japan, pp 121–121

Tuttle MP, Al-Shukri H, Mahdi H (2006) Very large earthquakes centered southwest of the New Madrid Seismic Zone 5,000–7,000 years ago. Seismol Res Lett 77:755–770

Youd TL, Idriss IM, Andrus RD, Arango I, Castro G, Christian JT, Dobry R, Finn WDL, Harder LF Jr, Hynes ME, Ishihara K, Koester JP, Liao SSC, Marcusion WF III, Martin GR, Mitchell JK, Moriwaki Y, Power MS, Robertson PK, Seed RB, Stokoe KH (2001) II: Liquefaction resistance of soils: summary report from the 1996 NCEER and 1998 NCEER/NSF workshops on evaluation of liquefaction resistance of soils. J Geotechn Geoenviron Eng 127(10):817–833